ACS OMEGA

http://pubs.acs.org/journal/acsodf

Article

Digital Microfluidics Chips for the Execution and Real-Time Monitoring of Multiple Ribozymatic Cleavage Reactions

Alen N. Davis, Kenza Samlali, Jay B. Kapadia, Jonathan Perreault, Steve C. C. Shih, and Nawwaf Kharma*

Cite This: *ACS Omega* 2021, 6, 22514−22524

Read Online

ACCESS | Metrics & More | Article Recommendations | Supporting Information

ABSTRACT: In this paper, we describe the design and performance of two digital microfluidics (DMF) chips capable of executing multiple ribozymatic reactions, with proper controls, in response to short single-stranded DNA inducers. Since the fluorescence output of a reaction is measurable directly from the chip, without the need for gel electrophoresis, a complete experiment involving up to eight reactions (per chip) can be carried out reliably, relatively quickly, and efficiently. The ribozymes can also be used as biosensors of the concentration of oligonucleotide inputs, with high sensitivity, low limits of quantification and of detection, and excellent signal-to-noise ratio. The presented chips are readily usable devices that can be used to automate, speed up, and reduce the costs of ribozymatic reaction experiments.

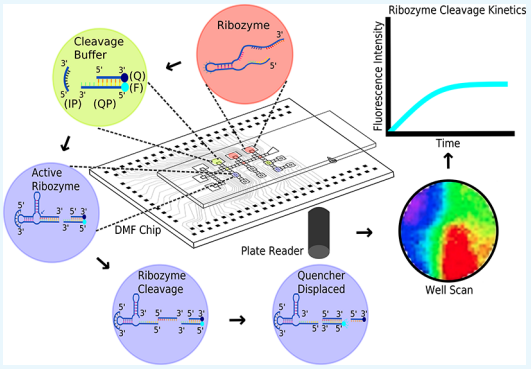

INTRODUCTION

With the advent of microfluidics technology, many devices have been developed to automate many biochemical reactions in small devices.[1−3] Such microstructured devices have also been used for a variety of applications including point-of-care medical diagnosis and the evolution of enzymes.[4,5] Among the different microfluidic platforms, the most prominent are the channel-based devices, which perform experiments by transporting reagents and samples, through a system of enclosed microchannels, as streams of fluids.[6−8] These systems also rely on molecular diffusion to mix the reagents. In a different approach, called droplet-in-channel microfluidics, the reagents are formed into droplets using immiscible fluids or air−liquid droplet systems.[9,10] These droplets are diffused (passively or actively) and mixed by chaotic advection.[11] The assayed droplets can also be easily sorted and stored for further analysis. A newer paradigm of microfluidics is digital microfluidics (DMF) systems, which follow the principles of electrowetting to implement biochemical workflows.[12−14] DMF platforms also handle reagents as droplets but on an array of electrodes rather than inside a microchannel system. These electrodes are actuated to move, split, dispense, merge, and mix reagent droplets on the DMF chip, facilitating the automation of biochemical reactions.[15−17]

Many enzymatic assays have been implemented on microfluidic devices, demonstrating the benefits of automating these reactions on such platforms.[6,18−20] These platforms enable experiments to be performed at lower volumes (μL or less), reducing reagent usage and mitigating losses due to sampling.[21,22] Often, when experiments are performed in microdroplets, reactions proceed at a higher rate,[8,21,22] thereby lowering analysis times and reducing monetary and labor costs. Additionally, such platforms can generate multiple analytes or microreactors on a single chip, facilitating the development of ultra-high-throughput systems.[21,23] Ideally, experiments on microfluidics systems would have greater sensitivity, dynamic range, and flexibility than other automation techniques. One such experiment used a microfluidic microprocessor for DNA lesion repair analysis, exhibiting a higher dynamic range while retaining the sensitivity exhibited by other macroscale methods.[24] In another experiment, a DMF platform was developed to successfully perform homogeneous enzymatic analysis with better sensitivity than other techniques and without sacrificing dynamic range.[25] Moreover, the portability and flexibility of these platforms when coupled with detection mechanisms such as fluorescence have made it easier to interface the devices with machines such as plate readers to automate entire experiments.[26]

Ribozymes are enzymes composed of ribonucleic acid (RNA) molecules capable of catalyzing specific biochemical reactions within cells and *in vitro*. These molecules excise themselves[27] or a substrate[28] upon the formation of a catalytic nucleotide core. This led many researchers to study and

Received: April 18, 2021
Accepted: July 22, 2021
Published: August 25, 2021

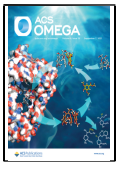

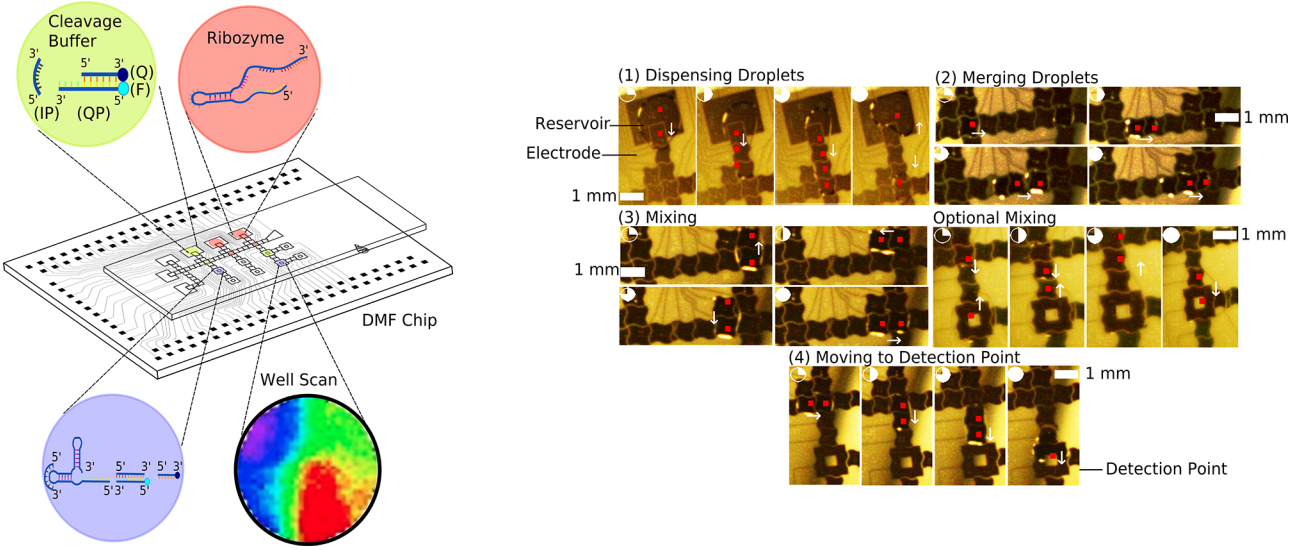

Figure 1. Overview of the ribozyme cleavage assay on a digital microfluidics (DMF) chip. On the DMF device, the ribozyme cleavage experiment is carried out in four steps, which are depicted in screenshots of different frames from a video of the experiment, where the red dots indicate the electrodes actuated in each frame. (1) First, a ribozyme-containing droplet (0.625 μM) and another containing a cleavage buffer (1.25×) are dispensed from their respective reservoirs by splitting (15 kHz, 178 V_{rms}). The ribozyme used in the experiment is an inducible *cis*-acting hammerhead ribozyme (HHR). The cleavage buffer contained a 6.25 μM input strand (IP, a ssDNA to activate the ribozyme) and a quenched probe (QP) composed of two ssDNA strands, one with Cy5 fluorophore (F) and the other with a black hole quencher (Q). (2) Next, the dispensed droplets are moved closer to each other and then merged. (3) The merged droplets are mixed by actuating four electrodes to move the droplets in a loop three times. (4) Finally, the assayed droplet is driven to the detection point for measurement. Optionally, the experiment can also be carried out by merging a dispensed ribozyme-containing droplet with an already pipetted droplet of cleavage buffer at the detection point. The merged droplet can then be mixed by moving it back and forth across the detection point three times. In the assayed droplet, the ribozyme cleaves itself after folding into an active hammerhead ribozyme (HHR) upon binding to the input strand. The cleaved-off RNA strand binds to the probe displacing the quencher, allowing the probe to fluoresce. Hence, measuring the fluorescence intensity reflects the amount of cleaved-off RNA strand that actually detaches from the ribozyme. The fluorescence of the assay is read by well-scanning the DMF device using a plate reader.

monitor the cleavage kinetics of different ribozymes.[29−34] Furthermore, many artificial ribozymes were designed for use in various fields, including therapeutics, as biosensors of small molecules and as computational units in RNA-based digital circuits.[35−38] Conventionally, the progress of a ribozyme cleavage reaction is reported using radioactivity or fluorescence.[29−34] When performed on the bench, these experiments use large volumes of reagents, various consumables (such as tubes, plates, and pipette tips), and a fair bit of skilled labor. Some of these experiments are performed in multiple steps[37] and require additional pipetting. These make such reactions prone to contamination and pipetting errors, which would be reduced by automation. A recent experiment exploited a droplet-based microfluidics system to isolate and select efficient ribozymes from a gene library and studied the catalytic activity of efficient ribozymes under multiple-turnover conditions.[39] However, these techniques lack tools for automated testing and real-time quantitative monitoring of ribozyme cleavage assays.

Compared to channel microfluidics, droplets on a DMF chip can be individually addressed and can be programmed to handle multiple droplets, allowing for the translation of multistep protocols onto the device.[40,41] DMF devices can also be integrated with software and electronics, which can generate or respond to feedback based on electrical, visual, or temperature signals.[42,43] Moreover, the arrays of electrodes make any DMF device reconfigurable, as a wide variety of droplet motions and functions can be achieved without chip redesign. This makes DMF an attractive platform for the automation of ribozyme cleavage reactions.

Here, we demonstrate the design and use of DMF devices to carry out ribozyme cleavage reactions and monitor the kinetics of these reactions in real time. For this purpose, we study the activity of an inducible *cis*-acting hammerhead ribozyme (HHR) due to the precisely described sequence and structure of HHR and the ease of generation of ribozymes in general.[30,44,45] The experiment uses a toehold mediated strand displacement reaction (SDR) to monitor the cleavage of the ribozyme by reading the resulting fluorescence.[46]

The study presents the successful implementation of multiple ribozyme cleavage reaction experiments on DMF chips. Viewed as biosensors, the results exhibit the greater sensitivity and lower limit of detection of DNA, when using these ribozymes on a DMF chip, relative to wells (of a well-plate). This research provides evidence that the DMF technology facilitates ribozymatic experimentation at the microscale without regular (often noisy) intraexperiment sampling or postexperiment polyacrylamide gel electrophoresis. This provides ribozymatic experimenters with a potent tool that would automate, speed up, and potentially lower the cost of their lab work.

RESULTS AND DISCUSSION

Design of a Digital Microfluidics Platform for Ribozyme Cleavage Reactions. Digital microfluidics (DMF) platforms have found their application in automating a variety of enzymatic reactions[6,19,25,47,48] and were monitored using luminescence[49] and fluorescence.[25] Ribozyme cleavage reactions are one type of such enzymatic reactions[50] and can similarly be analyzed by reading fluorescence intensities.[34,51,52]

https://doi.org/10.1021/acsomega.1c00239
ACS Omega 2021, 6, 22514−22524

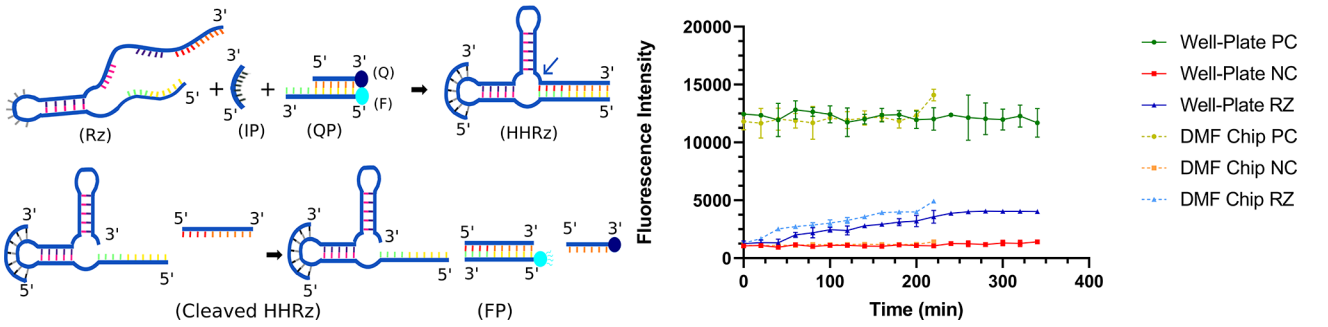

Figure 2. Comparison of the ribozyme well-plate and DMF chip assay. Monitoring the cleavage of the ribozyme was done by reading the fluorescence intensities resulting from the experiments performed in a well-plate and DMF chip. In the experiments, a solution (or droplet) of the ribozyme (Rz) (0.5 μM) is mixed with a solution containing the cleavage buffer with a single-stranded DNA input (IP) (5 μM) and a quenched probe (QP) (0.5 μM). The input strand (IP) binds to the ribozyme, inducing it to fold into an active hammerhead ribozyme (HHRz). In the active state, the ribozyme cuts itself at a position indicated by the arrow. The small RNA strand (output strand) that leaves the ribozyme after cleavage displaces the quencher and binds to the probe, rendering it fluorescent. The fluorescence intensities are read every 20 min and plotted against time. This shows the amount of output strand that leaves the ribozyme and binds to the probe (FP) over time. The continuous and dotted lines correspond to the experiments in the well-plate and on the chip, respectively. In addition to the ribozyme assay (RZ) (samples, n = 3, standard deviation, σ_{DMF} = 178, $\sigma_{well\text{-}plate}$ = 551), the experiments had positive (PC) and negative controls (NC). For NC, a quenched probe (0.5 μM) is used (n = 3, σ_{DMF} = 30, $\sigma_{well\text{-}plate}$ = 90). For PC, a strand displacement reaction using an ssDNA strand (0.5 μM) equivalent to the expected cleaved-off output RNA strand is used to displace the quencher from the probe (n = 3, σ_{DMF} = 471, $\sigma_{well\text{-}plate}$ = 972).

In this work, we designed a digital microfluidics chip to carry out a cleavage reaction of an inducible *cis*-acting hammerhead ribozyme (HHR). The chip also served as a platform to monitor ribozyme cleavage by reading the fluorescence intensity of a quenched probe, where the cleaved-off RNA strand binds to the probe displacing the quencher, allowing the probe to fluoresce.

The chip was designed to carry out six ribozymatic reactions and two control reactions on the same chip by merging ribozyme-containing droplets with droplets of the cleavage buffer and quenched probe (Figure 1). For this reason, the design had six reservoirs for dispensing droplets containing the ribozyme and cleavage buffer. The device also had eight detection areas to isolate and monitor the six assayed droplets along with the two controls: a negative and a positive control. In addition to this, three mixing areas composed of four electrodes were included in the chip. The interelectrode spacing (60 μm) was made to be twice the thickness of the wiring (30 μm) because some of the inner electrodes were connected to the contact pads through the spacing between the electrodes (Figure S4). Moreover, the electrode edges were shaped as "skewed-waves," which facilitated successful droplet movements across the DMF device. Studies have confirmed that square or rectangular electrodes often cause droplets to be stranded, seizing the droplet motion on the chip.[53] Comb, zig-zagged, or crescent shapes are also said to have solved the problem.[4,54] However, regions with pointy edges and high electric fields (>108 V/cm) are known to cause a dielectric breakdown,[55] while "skewed-wave" edged electrodes have been proven to resolve this problem.[26]

Droplet motion on the chip was achieved by actuating the electrodes for 0.7 s at a voltage of 178 V (15 kHz sine wave). To dispense droplets, a larger droplet was initially stretched by actuating four electrodes from the reservoir. After that, the third electrode was switched off, forcing a small droplet to separate from the larger droplet (Figure 1). When 2.5 μL of the reagent was pipetted on to the reservoir, the actuation of electrodes (surface area = 4 mm^2) dispensed droplets of the size of 0.5 $\pm$ 0.08 μL (n = 10). The dispensed droplets were merged and mixed at the mixing area by activating four electrodes in loops three times (Figure 1).

During the preliminary experimentation, ribozyme-containing droplets were moved across the chip and were reproducible without damaging the electrodes or the dielectric. However, the cleavage buffer droplets, which also contained the input ssDNA and the quenched probe, often failed to move across the chip and sometimes generated electrolysis (i.e., dielectric burnout) as we further increased the potential to move the droplet. When the droplets are static on the device, droplets start to stick onto the hydrophobic surface. Studies have shown that droplets with high alkaline content often caused significant biofouling,[25] which could be the same for the cleavage buffer droplet, as it contains a high salt content. Adding surfactants to such solutions have proven to be effective even without any filler oil.[26] Hence, 0.05% Tetronic 304 was added to the aqueous cleavage buffer. Although the surfactant resulted in the improved movement of the cleavage buffer droplets (similar to our previous study[26]), it was observed in this study that the droplets had left traces along their paths, which made chip reuse quite difficult. Therefore, the reactions were done at larger volumes (2.5 μL) by directly dispensing cleavage buffer droplets on the detection points (to enable reusability of the chip) and then merging them with ribozyme-containing droplets (Figure 1).

To measure fluorescence intensities, a previously established protocol[26,43] was followed. After executing the experiments on the DMF chip, the device was carefully removed from the automation system and placed on a flat black-sided clear-bottom 384-well-plate while carefully aligning the detection points with the wells. Five wells around the chip were filled with 30 μL of DI water to reduce evaporation because the DMF chip fluorescence intensities of all the assays, including the controls, were found to increase significantly after 60 min. Previous experiments[13,56] have used filler oil to prevent DMF chip droplet evaporation, but this can cause the probe to leak into the oil, resulting in cross-contamination.[57] The well-plate was covered by a lid, sealed using parafilm, and then scanned in a plate reader (ClarioSTAR) at 37 °C. The machine takes up to 20 min to scan the entire chip. Thus, readings correspond to

https://doi.org/10.1021/acsomega.1c00239
ACS Omega 2021, 6, 22514−22524

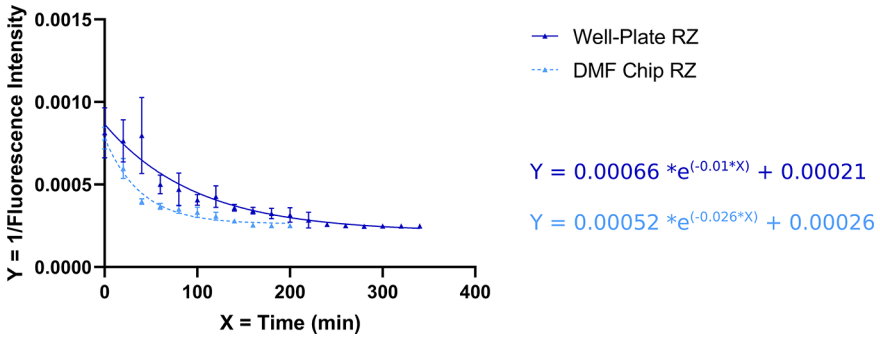

Figure 3. Well-plate and DMF chip kinetics of the ribozyme cleavage assay. The inverse of fluorescence intensities of the ribozyme cleavage assay (AS) was plotted against time to express the fluorescence readings as a decaying function of the uncleaved ribozyme. The change in the fluorescence intensities over time is expressed as a one-phase decay equation of the form $Y = (Y_0 - \text{Plateau}) \times e^{(-KX)} + \text{Plateau}$, where Y = the amount of the uncleaved ribozyme, X = the time in minutes, K = the rate of the reaction, Y_0 = the initial value of Y, and Plateau = the value of Y at which the reaction reaches a plateau (K_{DMF} = 0.026, $K_{well\text{-}plate}$ = 0.01, Y_0^{DMF} = 0.00052, $Y_0^{well\text{-}plate}$ = 0.00066, $Plateau_{DMF}$ = 0.00026, and $Plateau_{well\text{-}plate}$ = 0.00021).

fluorescence intensities at 20 min intervals, starting from the moment the well-plate is placed in the plate reader. From the resultant matrix of pixels (Figure S5A), the regions corresponding to the detection points were selected, and the highest fluorescence intensity of each detection point was recorded. After 180 min, the positive control, a strand displacement reaction, exhibited an average highest fluorescence reading of 12,250 units (Figure S5B). The assayed ribozyme reported a fluorescence intensity of 4900 units, while a low fluorescence level of 1530 units was recorded for the negative control (a quenched probe).

The results demonstrated that the designed DMF chip could manipulate the droplets containing ribozymes and the cleavage buffer with no or minimal biofouling. In this way, the ribozyme cleavage reaction could be initiated on the DMF by merging and mixing the ribozyme and buffer droplets. Moreover, the progress of the reaction could also be monitored by reading the fluorescence.

Monitoring of Ribozyme Cleavage Kinetics on a DMF Chip. The research primarily aims to demonstrate the feasibility of performing ribozyme cleavage experiments on DMF platforms. To achieve this, a cleavage assay using an inducible *cis*-acting hammerhead ribozyme (HHR) was carried out both in a well-plate and on a DMF chip, and the results were compared. The cleavage was then monitored by reading a fluorescent signal generated by the probe once the quencher has been displaced by the ribozyme's output strand.

The well-plate and DMF chip experiments were performed following the same workflow as detailed in the previous section, after which the fluorescence intensities were read regularly every 20 min. In addition to the cleavage assay, the experiments had a positive control (a strand displacement reaction) and a negative control (a quenched probe).

The fluorescence intensities of both the well-plate and DMF chip experiments were plotted against time (Figure 2). The change in fluorescence intensities over time was then analyzed by fitting a line to the readings using linear regression (Figure S6). The line fit to the readings from the positive control (PC) both in the well-plate and on the chip had smaller slopes (Student's t test, $P > 0.05$, $PPC_{well\text{-}plate} = 0.78$, $PPC_{DMF} = 0.78$), indicating no or a small change in fluorescence during the experimentation ($SlopePC_{well\text{-}plate} = -1 \pm 3.5$, $SlopePC_{DMF} = 0.85 \pm 3.1$). Similarly, a small change in the fluorescence intensities (Student's t test, $P > 0.05$, $PNC_{well\text{-}plate} = 0.3$, $PNC_{DMF} = 0.08$) was observed for the negative controls (NC) in the well-plate and on the chip with smaller slopes ($SlopeNC_{well\text{-}plate} = 0.53 \pm 0.51$, $SlopeNC_{DMF} = 0.33 \pm 0.18$), whereas the line fit to the assayed ribozyme (RZ) had a positive slope (Student's t test, $P < 0.05$, $PRZ_{well\text{-}plate} < 0.0001$, $PRZ_{DMF} < 0.0001$) both on the chip and in the well-plate, indicating an increase in the fluorescence intensities over time on these platforms ($SlopeAS_{well\text{-}plate} = 10.30 \pm 1.6$, $SlopeAS_{DMF} = 11.2 \pm 0.8$). This rise in fluorescence indicated that, in the presence of the inducing DNA strand, the HHR folded into an active ribozyme, leading to self-cleavage. Hence, the cleaved-off RNA strand displaced the quenching strand and hybridized to the probe, allowing the probe to fluoresce, in both the DMF chip and the well-plate. Both well-plate and chip assays displayed similar trends over time. The results show no significant difference between the two assays (Student's t test, $P > 0.05$, $PAS_{DMF\_vs\_well\text{-}plate} = 0.054$). This provides good evidence that the ribozyme cleavage experiment was reproducible on the DMF chip. Moreover, we noticed that the assay readings from the DMF chip exhibited a smaller standard deviation than that of the well-plate experiments (Student's t test, $P > 0.05$, $PSD_{DMF\_vs\_well\text{-}plate} = 0.0054$). The errors in well-plate assays could have been introduced due to pipetting and other human errors, which are minimized on a DMF platform. This was verified by measuring the signal-to-noise ratio (SNR) for both DMF chip and well-plate readings. The signal-to-noise ratio (SNR) was calculated by dividing the arithmetic mean of the fluorescence readings of the triplicates for each assay by their standard deviation. At the end of 180 min, the fluorescence readings of the assay on the DMF chip exhibited an improved SNR compared to the well-plate readings ($SNR_{well\text{-}plate} = 8.95$, $SNR_{DMF} = 18.95$, Student's t test, $P < 0.05$, $P_{SNR} = 0.0023$). These calculations showed that the DMF technology can provide more reliable platforms to execute ribozymatic assays, a property that was also observed in previous studies.[25]

The inverse of fluorescence intensities from the readings can also help us determine the decay of the uncleaved ribozyme over time, providing insight into the ribozyme kinetics. The ribozyme was consumed during the reaction, and hence, the rate of reaction was calculated from the amount of the uncleaved ribozyme at different time points according to a first-order reaction.[29] Therefore, the kinetics of ribozyme cleavage can be analyzed using a one-phase decay equation[33]

https://doi.org/10.1021/acsomega.1c00239
ACS Omega 2021, 6, 22514−22524

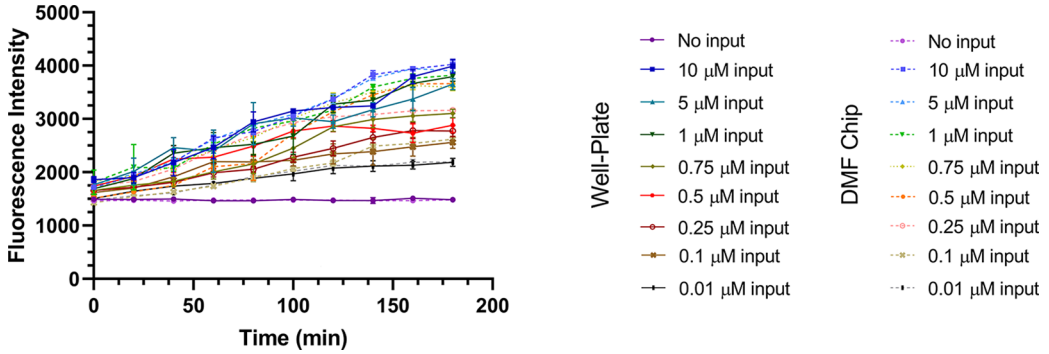

Figure 4. Monitoring the progress of the ribozyme cleavage reaction with varying input concentrations. At first, the ribozyme cleavage assays are performed both on the DMF chip and in a well-plate at different input ssDNA concentrations (10, 5, 1, 0.5, 0.25, 0.1, and 0.01 μM and zero input). Then, fluorescence intensities are read every 20 min and plotted against time for 180 min to observe the progress of the cleavage reaction (n = 3, $\sigma_{DMF}^{no\ input}$ = 4, $\sigma_{well\text{-}plate}^{no\ input}$ = 13, σ_{DMF}^{10} = 76, $\sigma_{well\text{-}plate}^{10}$ = 132, σ_{DMF}^{5} = 41, $\sigma_{well\text{-}plate}^{5}$ = 105, σ_{DMF}^{1} = 24, $\sigma_{well\text{-}plate}^{1}$ = 590, $\sigma_{DMF}^{0.75}$ = 64, $\sigma_{well\text{-}plate}^{0.75}$ = 82, $\sigma_{DMF}^{0.5}$ = 30, $\sigma_{well\text{-}plate}^{0.5}$ = 130, $\sigma_{DMF}^{0.25}$ = 48, $\sigma_{well\text{-}plate}^{0.25}$ = 100, $\sigma_{DMF}^{0.1}$ = 34, $\sigma_{well\text{-}plate}^{0.1}$ = 112, $\sigma_{DMF}^{0.01}$ = 33, and $\sigma_{well\text{-}plate}^{0.01}$ = 75).

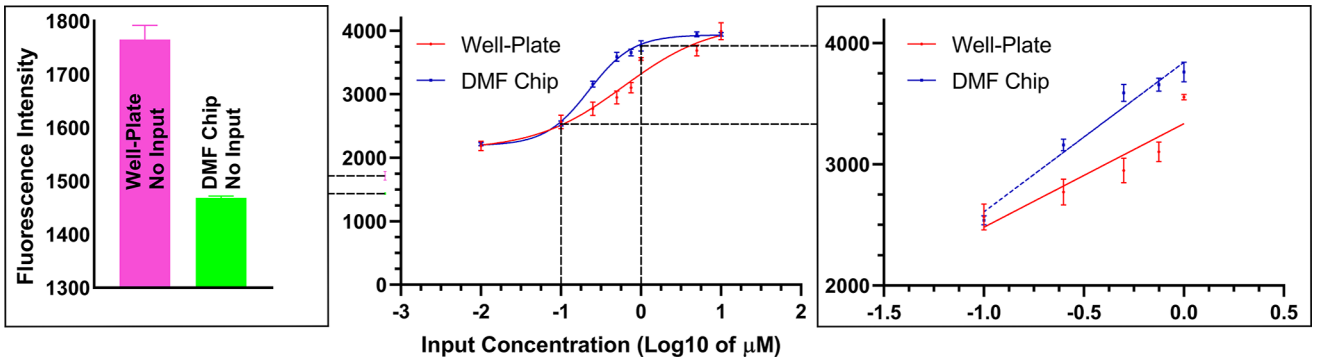

Figure 5. Analysis of ribozyme as a biosensor by activating the ribozyme with varying input concentrations. After carrying out the ribozyme cleavage assays at different input concentrations, the end point (180 min) fluorescence readings of each assay are noted and plotted as a function of the input concentration (in Log10 scale). A four-parameter logistic (4-PL) sigmoidal model is fit to the graph, from which a near-linear region is extracted for further analysis (between 0.1 and 1 μM). A linear regression model is fit to the extracted region and used to calculate the sensitivity and limit of detection (LoD) of the ribozyme as a sensor of an input ssDNA strand (LoD_{DMF} = 1475 and $LoD_{well\text{-}plate}$ = 1845). Additionally, the end point fluorescence intensities of the assays without input are also measured to calculate the limit of quantification (LoQ) of the ribozyme (LoQ_{DMF} = 0.025 and $LoQ_{well\text{-}plate}$ = 0.31).

(Figure 3). The inverse of fluorescence intensities was plotted against the time and fitted with a one-phase decay equation ($R2_{well\text{-}plate}$ = 0.84 and $R2_{DMF}$ = 0.95) (Figure 3). The reactions proceeded at a rate of k_{obs}well-plate = 0.01 ± 0.003 min^{-1} in the well-plate and k_{obs}DMF = 0.026 ± 0.005 min^{-1} on the chip. Eventually, the amount of the uncleaved ribozyme reached a plateau (Table S5).

Interestingly, it was also observed that the rate of cleavage of the ribozyme on the DMF chip (k_{obs}DMF = 0.026 ± 0.005 min^{-1}) was ~2.5 times that of the well-plate cleavage rate (k_{obs}well-plate = 0.01 ± 0.003 min^{-1}). It was hypothesized that this was due to the higher surface-area-to-volume (SAV) ratio of reaction-holding droplets in the DMF platform. The increased SAV can lead to improved intermolecular collisions, thereby increasing the rate of the reaction.[58,59] The higher rate of cleavage could have also been due to molecular crowding caused by surfactant molecules (Tetronic 304), as discussed in other studies.[60]

The results from the above experiments demonstrated the successful deployment of ribozyme cleavage experiments on a DMF chip. DMF is a promising technology that could provide platforms to carry out such ribozymatic experiments in an automated fashion at a higher rate and using lower volumes of reagents, leading to a significant reduction in experimental costs.

Ribozyme as a Biosensor on a DMF Chip. Ribozymes have found their application as biosensors for the detection of a variety of organic molecules including antibiotics, specific nucleic acid sequences, peptides, proteins, and metal ions.[36,61−63] In our own experiment, a ribozyme was used to detect the concentration of input DNA strands. Here, we show that a DMF protocol can facilitate an experiment to validate the sensitivity and limit of detection of a ribozyme-based DNA biosensor.

Ribozyme cleavage experiments were performed both on the DMF chip and in a well-plate at different input concentrations (10, 5, 1, 0.75, 0.5, 0.25, 0.1, and 0.01 μM and no input) following the protocols described in the previous section. For each input concentration, the fluorescence intensities were read regularly every 20 min for a total period of 180 min, showing the progress of cleavage over time (Figure 4).

To examine the sensitivity of the ribozyme as a sensor, a calibration (or standard) curve was generated by plotting the end point (180 min) fluorescence readings for each assay against the input concentration on a logarithmic scale (Figure 5). These results from both the chip and well-plate assays followed a sigmoidal curve (Table S6). Next, a linear

https://doi.org/10.1021/acsomega.1c00239
ACS Omega 2021, 6, 22514−22524

regression model was fit to a near-linear region (between 0.1 and 1 μM) of the sigmoidal curve. As shown in previous studies, the slope of the fitted line indicated the sensitivity of the biosensor.[65] The fitted lines for both the chip and well-plate displayed a positive slope ($SlopeRzB_{well\text{-}plate}$ = 850 ±120 and $SlopeRzB_{DMF}$ =1230 ±71). However, the line fitted to the readings from the chip had a steeper slope and smaller standard error showing a higher sensitivity on the DMF platform than in the well-plate (Student's t test, $P < 0.05$, P value = 0.0087). The higher sensitivity on the DMF chip could be due to the high SAV ratio of reaction-holding droplets on the DMF platform.[58,59] Although its sensitivity was lower, the linear dynamic range of the well-plate assay was twice as large as that of the DMF assay, which can be assigned to the limited number of dilutions performed on our DMF device. A simple solution to that problem is increasing the throughput of future device designs.[26,40] This allows the user to run multiple experiments with different dilutions to identify (and simultaneously get the results of the experiment with) the optimal dilution factor for his/her particular application.

In addition, parameters of the ribozyme-based biosensor, such as the limit of detection (LoD) and limit of quantification (LoQ), were calculated. These parameters further characterize the ribozyme as a biosensor.[64,65] LoD indicates the lowest input concentration in the assay at which the detection can be differentiated from an assay with no input, whereas LoQ represents the concentration level of the input above which the quantitative results can be presented with confidence. LoD and LoQ were calculated using equations $blank_{mean} + 3 \times SD$ and $10 \times SD/S$, respectively, where $blank_{mean}$ is the mean fluorescence intensity of assays with no input ssDNA, SD is the standard deviation of the $blank_{mean}$, and S is the slope of the regression line.[66,67] The LoD of the experiments on the chip was observed to be ∼80% of that in the well-plate ($LoD_{well\text{-}plate}$ = 1845 and LoD_{DMF} = 1475). Similarly, the LoQ of the experiments on the chip was ∼8% of that in well-plate assays ($LoQ_{well\text{-}plate}$ = 0.31 and LoQ_{DMF} = 0.025). These low LoD_{DMF} and LoQ_{DMF} values showed that the ribozyme performs better as a biosensor on the DMF chip than in the well-plate. The improvements to the detection limits of the ribozyme-based biosensor could also be due to the higher SAV ratios on DMF chips, also recorded in prior research involving microfluidic platforms.[68]

The above results demonstrated that the near-linear sections of the standard curves generated from the cleavage assays on the DMF chip and well-plate could be used to characterize ribozymes. These readings could also be utilized to describe the activity of ribozyme biosensors for the measurements of small input DNAs and RNAs. Based on the results from the experiments, it was observed that the sensitivity and detection limits of ribozyme-based sensors could be improved when deployed on DMF platforms.

Multiple Ribozyme Cleavage Assays on a DMF Chip. Additionally, a second DMF chip was designed to facilitate simultaneous experimentations via the execution of multiple reactions on the same chip. Although the first chip had eight detection points, some of these fell along the paths of other detection points. Hence, the reagent droplets tend to leave traces and contaminate these detection points as they move across them, effectively limiting the number of experiments that can be done simultaneously to three.

The new chip consisted of 5 reservoirs to dispense reagents droplets; a 3 × 17 matrix of electrodes for moving, merging, and splitting the droplets; and 8 detection points for analyzing the assayed droplets. All the electrodes, detection points, and reservoirs had the same dimensions and had the same interelectrode spacing and wiring widths as the first chip (Figure S8). The device dispensed droplets of size = 0.51 ± 0.056 μL (n = 10) from 2.5 μL reagent droplets at the reservoirs. Experiments were carried out by dispensing ribozyme-containing droplets (∼0.5 μL) from the reservoirs and mixing and merging them with cleavage buffer droplets (2 μL) at the detection points following the same procedure used on the first chip.

The chip was successfully tested by carrying out two experiments. The first involved a ribozyme cleavage assay in triplicates (AS1, AS2, and AS3) with one positive control (PC, a strand displacement reaction) and one negative control (NC, a quenched probe). After performing the experiments on the chip, regular well-scans were taken every 4 min for 132 min (Figure S9), and the fluorescence intensities were plotted against time. In the second experiment, a ribozymatic experiment (AS) was performed on the new chip with one positive control (PC, a strand displacement reaction) and five negative controls. The negative controls included a quenched probe in the cleavage buffer (NC1), a buffer without $MgCl_2$ and input strand (NC2), a buffer with $MgCl_2$ (NC3), a buffer with input strand (NC4), and finally a buffer with a mutated input ssDNA and $MgCl_2$ (NC5). The assays followed the same steps as described in the section DMF Ribozyme Cleavage Assay in methodology, and regular fluorescence intensities of the assays were read every 9 min and plotted over time (Figure S10).

The results displayed the feasibility of carrying out multiple ribozymatic experiments, simultaneously, on one DMF chip. We also note that the DMF technology has the advantages of dynamic processing in contrast to well-plates, which are static platforms. DMF devices allow users to address individual samples without the need for micro-pumps, valves, or mixers. They are also connected to programmable devices such as micro-controllers or computers. This offers the potential to standardize ribozymatic assays, such as the one employed in our study. Together with the increased sensitivity, we have demonstrated the reliability of our DMF platform for ribozymatic assays. Such DMF platforms allow researchers to automate the initiation of multiple ribozyme cleavage assays at the same time while monitoring the progress of these reactions in real time. Due to the flexibility of the electrode design, DMF chips can be designed to accommodate multiple replicates, and several identical DMF chips can be fabricated and operated in parallel, which further increase the number of experiments. This increases the throughput of the experimental platform and reduces both labor costs and waiting time to final data collection.

MATERIALS AND METHODS

Reagents and Materials. Unless specified otherwise, all general-use chemicals and kits were purchased from Sigma-Aldrich (St. Louis, Missouri). The primary reagents for the experiments included a stock of cleavage buffer (1.25× concentrated) and a solution of the ribozyme (2.5 μM). The buffer was composed of 125 mM NaCl, 62.5 mM Tris (7.5 pH), 31.25 mM KCl, 12.5 mM $MgCl_2$, 0.0625% Tetronic 304, 2.5 μM quenched probe, and 6.25 μM (or as specified in the text) single-stranded DNA (ssDNA, an input strand to activate the ribozyme).

https://doi.org/10.1021/acsomega.1c00239
ACS Omega 2021, 6, 22514−22524

Ribozyme Transcription. Ribozymes were transcribed from a DNA template (Figure S1) produced by carrying out an assembly PCR of overlapping primers. The primers F1, F2, R1, and R2 (Table S1) for the ribozyme were generated using the tool Primerize.[69] A PCR mixture composed of primers F1 (2 μM), R1 (0.2 μM), F2 (0.2 μM), and R2 (2 μM); Taq polymerase (hotStar Taq Plus from QIAGEN) with its reaction buffer at 1×; Q-solution (1× from QIAGEN); 0.2 mM of dNTPs (DGel electrosystem); and milli-Q water was prepared at a fixed volume of 100 μL. The reaction mixture was denatured at 95 °C for 15 min and subjected to 15 cycles of 30 s denaturation at 95 °C, 30 s annealing at 50 °C, and 30 s extension at 72 °C. Finally, the PCR product was ethanol precipitated.

For 1 mL *in vitro* RNA synthesis reaction, 10 PCRs (100 μL each) were mixed, precipitated, and resuspended in 150 μL of milli-Q water. The reaction mixture for *in vitro* RNA synthesis contained 80 mM HEPES (pH 7.5), 24 mM $MgCl_2$, 40 mM dithiothreitol, 2 mM spermidine, 6 μg/mL T7 polymerase, 150 μL of the resuspended PCR product (10 reactions), 2 mM rNTPs, 1× pyrophosphatase (Roche Diagnostics), and 200 U (40 μL) of RiboLock (Thermo Fisher Scientific). The mixture was incubated for 30 min at 37 °C. Immediately after, the mixture was treated with 10 U of DNase (New England Biolabs) and left for incubation at 37 °C for 30 min. After extracting the RNA using phenol−chloroform, the aqueous phase was ethanol precipitated. Purification of the RNA was done in a 10% denaturing (8 M urea) polyacrylamide gel, and UV-shadowing was used to visualize bands. The highest band on the gel (as there was some level of cleavage during transcription) was cut out and eluted in 0.3 M NaCl overnight at 4 °C. The eluent was ethanol precipitated and resuspended in nuclease-free water.

Preparation of the Probe. A probe was designed for detecting ribozyme self-cleavage that consists of two single-stranded DNA (ssDNA) molecules, namely, an F-strand and a Q-strand (Figure S2). The 5′ end of the F-strand was linked to a fluorophore (Cy5), while a Black Hole Quencher (BHQ-3) was attached to the 3′ end of the Q-strand. The two strands were purchased from Alpha DNA (Montreal, Canada).

The preannealed quenched probe was prepared in a 1.25× cleavage buffer (125 mM NaCl, 62.5 mM Tris−HCl pH 7.5, and 31.25 mM KCl) with the F-strand (0.625 μM) and Q-strand (0.7 μM). The mixture was incubated in a thermocycler (Biorad T100) and underwent 3 min denaturation at 95 °C, 15 min annealing at 50 °C, and 15 min annealing at 37°C. The final mixture was prepared in bulk and stored at − 20 °C. Before usage, a solution of surfactant Tetronic 304 (Sigma-Aldrich) (0.05% per 10 μL) was also added to the mixture.

Automation System for the DMF Chip. The automation system was composed of an in-house Python 2.7 software[70] to control an Arduino Uno microcontroller (Adafruit) driven control board. A 15 kHz sine wave output from a function generator (Agilent Technologies) was amplified by a PZD-700A amplifier (Trek Inc.). The amplified signal was used as the driving input with a voltage of 178 V (V_{RMS}), which is delivered to a control board that passes it on to the electrode, bypassing through high-voltage optocouplers on the control boards. An I/O expander (Maxim 7300, Digikey) controlled the logic state of each solid-state switch (high or pulled-to-ground) through I2C communication. The control board was interfaced with pogo pins, where the switches deliver a high-voltage potential (or ground) to the contact pads on the chip. The top plate of the device was grounded. The hardware assembly and instructions to install the open-source codes are detailed on the Shih lab repository (available on request).

The droplets on the chip were driven by actuating the electrodes. A voltage of V_{RMS} (178 V) was applied to switch the electrodes on. The protocol file associated with the automation system is updated with the parameters for each sequential actuation of electrodes, required by the automation system. Each sequence can be further configured (electrode pulse time and period) and can be initiated through the command line.

DMF Fabrication. A standard photolithography method, as previously reported,[71] was used for the fabrication of the digital microfluidics devices. A photomask was designed in AutoCAD 2018 (AutoDesk) and printed on a transparency film (CAD/Art services, Bandon, OR). A glass substrate precoated with an S1811 photoresist (Telic) was exposed to UV (8 s) under the photomask on a Quintel Q-4000 mask aligner (Neutronix Quintel). Substrates were developed using the MF321 developer (Rohm and Haas), baked (115 °C, 1 min), and etched in a CR-4 chromium etchant (OM Group). The remaining photoresist was stripped using an AZ-300T stripper (2 min). After rinsing with deionized (DI) water and air drying, the substrates were silanized (DI water, 2-propanol, and (trimethoxysilyl)-propyl methacrylate; 50:50:1) for 15 min.

Electrode contact pads were covered with Kapton tape (Kapton), after which a dielectric, 7 μM Parylene-C (Specialty Coating Systems), was deposited on the substrates using an SCS Labcoter 2 PDS 2010 (Specialty Coating Systems). Finally, a top plate was cut to size from an ITO (indium tin oxide) precoated glass slide (cat. no. CG-61IN-S207, Delta Technologies). A hydrophobic layer of 1% Teflon-AF (FC40) was deposited on both the bottom substrate and the top plate using a Laurell spin coater (North Wales) (500 rpm, 100 rpm/s, 30 s; 3000 rpm, 500 rpm/s, 60 s), after which the substrates were baked (160 °C, 10 min). The device was assembled by placing small stacks of two layers of double-sided tape (3M Canada) (each of thickness 70 μm) in between the bottom and top plates (Figure S4).

Well-Plate Ribozyme Cleavage Assay. In a black-sided flat clear-bottom 384-well-plate, 2 μL of the ribozyme (2.5 μM) was mixed with 8 μL of the cleavage buffer (1.25×) containing 6.25 μM input ssDNA and 12.5 mM $MgCl_2$. In addition, five wells near the assayed wells were filled with 30 μL of water to maintain the humidity within the well-plate. The plate was then covered with its lid and sealed using parafilm. The well-plate was inserted into the microplate reader ClarioSTAR (BMG Labtech) to take fluorescence readings every 20 min with 8 flashes at λ_{ex} = 647 nm and λ_{em} = 665 nm at 37 °C. The focal length and gain for the measurements were calibrated using a 10 μL solution of 0.5 μM fluorophore (Cy5) and was set to 6.4 mm and 1800, respectively.

DMF Ribozyme Cleavage Assay. The DMF substrate was cleaned up using RNAse away, IPA, and DI water and subsequently air-dried. After mounting the device onto the automation system, 2.5 μL of the ribozyme (2.5 μM) and 2 μL of the cleavage buffer (1.25×) were pipetted onto the reservoirs and detection points, respectively. The top plate was then placed on the chip and was connected to a ground wire. A droplet of ribozyme (~0.5 μL) was dispensed from the reservoirs, using a dispense electrode pattern, to the third electrode. This droplet was then moved toward the detection

https://doi.org/10.1021/acsomega.1c00239
ACS Omega 2021, 6, 22514−22524

point by sequentially actuating four electrodes between the electrode with the dispensed droplet and the detection point. The droplet containing the ribozyme was then merged with the droplet of the cleavage buffer at the detection point. The resulting droplet was moved up and down across the detection point by actuating four electrodes for 10 s to mix all the droplet contents.

After merging and mixing the droplets, the chip was carefully removed from the automation system and stacked on a Corning 384 well-plate (black and flat bottom). The detection points were aligned to the wells in the well-plate, and the wells surrounding the chip were filled with 30 μL of water. The well-plate was then covered with its lid and sealed using parafilm. This setup was inserted into the plate reader ClarioSTAR (BMG Labtech) to measure the fluorescence. Wells aligned to the detection points were scanned using a well-scanning program in the plate reader via a scan matrix (30 × 30 pixels, where each pixel represented 10 mm^2). The well-scans were taken regularly every 20 min at 37 °C with 8 flashes, a focal height of 15.80 mm, and a gain of 1800 (λ_{ex} = 647 nm and λ_{em} = 665 nm). From the scanned matrix, the region corresponding to the detection point was selected and the fluorescence was noted.

Data Analysis. The data analysis of the fluorescence readings was carried using Prism 8 (GraphPad Software). The droplet images were analyzed using ImageJ 1.52p (Fiji).

SUMMARY AND CONCLUSIONS

Ribozymes are used for many applications such as biosensing and as building blocks for genetic circuits. Thus, researchers have been keen on characterizing both the structure and function of ribozymes, in many cases, by analyzing their cleavage kinetics, using a variety of techniques.

In this study, we designed a digital microfluidics (DMF) device, or chip, to perform multiple ribozymatic cleavage reactions while monitoring their progress in real time. The chip used an in-house software to manipulate droplets containing the ribozyme, cleavage buffer, and quenched probe to ultimately initiate the cleavage reaction by mixing the droplets together. Hence, the single-stranded RNA output of the ribozyme's self-cleavage reaction displaces the quenching strand of the double-stranded DNA probe. This toehold mediated strand displacement reaction (TMSDR) allows us to indirectly monitor the progress of ribozyme self-cleavage in real time using a florescence measuring plate reader.

The results from the study show that ribozyme cleavage experiments are reproducible on DMF chips. Moreover, these cleavage reactions proceeded at a greater rate (~2.5 times) than equivalent well-plate assays. In addition, we generated a standard curve relating the level of fluorescence (of probe) to the concentration of the single-stranded DNA input (of the self-cleaving ribozyme). The curve showed that the ribozyme on the DMF chip exhibited a greater level of sensitivity (~45% more than that in the well-plate) to DNA input and a lower limit of quantification (LoQ_{DMF} = 0.025) and limit of detection (LoD_{DMF} = 1475) than the same ribozyme in a well-plate ($LoD_{well\text{-}plate}$ = 1845 and $LoQ_{well\text{-}plate}$ = 0.31). The experiments from the DMF chips also generated reliable fluorescence readings with a signal-to-noise ratio equal to twice as much that in the well-plate. We also designed and tested a second DMF chip that allows for the execution of up to eight parallel ribozyme cleavage reactions on the same chip (we carried out six experiments plus a positive and negative controls). Using multiple DMF chips is a swift and well-trodden path to scaling up, further, the number of simultaneous experiments.

The results from the ribozymatic experiments on the DMF devices exhibited a similar trend to those carried out in well-plates. This strongly suggests that the change in platform had no effect on the ribozyme's structure or functionality. Moreover, automating these experiments on DMF chips helps researchers perform multistep experiments involving ribozymes at lower volumes without additional sampling. However, scanning the DMF chips to read the emitted fluorescence was a time-consuming process. This made it difficult to measure the kinetics of faster ribozymes and to get their time course. Future studies could focus on improving the protocols for reading fluorescence on DMF chips over shorter intervals. Practicing rapid prototyping techniques for chip fabrication can also improve experimentation.

In brief, computer-controlled microfluidics devices offer ribozymatic researchers the ability to carry out multiple and different reactions using small volumes of reagents and involving minimal human intervention while reading the output of these reactions as they progress, obviating (for many but not all cases) the need for postreaction gels. This lowers the experimental costs and time while simultaneously increasing the quality of the harvested data in terms of greater sensitivity and signal-to-noise ratio as well as lower limit of quantification (LoQ) and limit of detection (LoD).

ASSOCIATED CONTENT

Supporting Information

The Supporting Information is available free of charge at https://pubs.acs.org/doi/10.1021/acsomega.1c00239.

Schematic representation of primerize assembly design (Figure S1); preparation of the quenched probe (Figure S2); side view of the digital microfluidics device (Figure S3); a schematic of the DMF chip and device operations to perform the ribozyme cleavage assay (Figure S4); on-chip fluorescence intensity measurements (Figure S5); analysis of change in fluorescence intensities in the ribozyme cleavage experiment (Figure S6); progress of ribozyme cleavage reaction at different input ssDNA concentrations (Figure S7); a schematic of a new DMF chip design to carryout multiple experiments (Figure S8); ribozymatic assay in triplicates on a DMF chip (Figure S9); multiple experiments performed simultaneously on a DMF chip (Figure S10); gel analysis of the ribozyme cleavage in the presence of input ssDNA oligonucleotide (10 μM) (Figure S11); quantifying the amount of cleaved-off strand that leaves the manganese activated ribozyme (Figure S12); ribozymatic assays on well-plate at lower volumes (Figure S13); primers are generated by the tool Primerize for the assembly of the ribozyme (Table S1); parameters of linear regression fit to the benchtop and on-chip negative controls (Table S2); parameters of linear regression fit to the benchtop and on-chip positive controls (Table S3); parameters of linear regression fit to the benchtop and on-chip assay (table S4); parameters of one-phase decay regression fit to the benchtop and on-chip ribozyme cleavage assay (Table S5); parameters of sigmoidal curve fit to the ribozyme cleavage assay on benchtop and on-chip experiments with different input concentrations (Table S6); and an estimation of the cost and time of

https://doi.org/10.1021/acsomega.1c00239
ACS Omega 2021, 6, 22514−22524

ribozymatic experiments on both well-plate and DMF chips (Table S7) (PDF)

Ribozymatic assay performed in triplicates (Video S1) (MP4)

Ribozyme assay with multiple controls (Video S2) (MP4)

AUTHOR INFORMATION

Corresponding Author

Nawwaf Kharma − *Department of Electrical and Computer Engineering, Concordia University, Montreal, Québec H3G 1M8, Canada; Centre for Applied Synthetic Biology, Concordia University, Montréal, Québec H4B 1R6, Canada*; Phone: (514) 848-2424 x3117; Email: nawafkharma@gmail.com

Authors

Alen N. Davis − *Department of Electrical and Computer Engineering, Concordia University, Montreal, Québec H3G 1M8, Canada*; orcid.org/0000-0002-6025-4526

Kenza Samlali − *Department of Electrical and Computer Engineering, Concordia University, Montreal, Québec H3G 1M8, Canada; Centre for Applied Synthetic Biology, Concordia University, Montréal, Québec H4B 1R6, Canada*

Jay B. Kapadia − *Department of Electrical and Computer Engineering, Concordia University, Montreal, Québec H3G 1M8, Canada*

Jonathan Perreault − *Centre for Applied Synthetic Biology, Concordia University, Montréal, Québec H4B 1R6, Canada; Armand-Frappier Health Biotechnology Center, Institut national de la recherche scientifique, Laval, Québec H7V 1B7, Canada*

Steve C. C. Shih − *Department of Electrical and Computer Engineering, Concordia University, Montreal, Québec H3G 1M8, Canada; Centre for Applied Synthetic Biology, Concordia University, Montréal, Québec H4B 1R6, Canada; Department of Biology, Concordia University, Montréal, Québec H4B 1R6, Canada*; orcid.org/0000-0003-3540-0808

Complete contact information is available at: https://pubs.acs.org/10.1021/acsomega.1c00239

Author Contributions

N.K., J.P., J.B.K., and S.C.C.S.H. designed the experiments. A.N.D. designed and fabricated the devices with the help of K.S. J.B.K performed the ribozyme transcription and purification. A.N.D. carried out the experiments on- and off-chip and analyzed the data with N.K., J.P., K.S., and S.C.C.S. A.N.D., K.S., and N.K. wrote the paper and prepared the figures. All the authors reviewed the final version of the manuscript before the final submission.

Notes

The authors declare no competing financial interest.

Jonathan Perreault is a junior 2 FRQS research scholar. Other funding, including for open access charge: NSERC [RGPIN-2019-06403]. Steve Shih thanks the Natural Sciences and Engineering Research Council (NSERC) (RGPIN-2016-06712), the Fonds de Recherche Nature et technologies (FRQNT) (No. 204862), and the Canadian Foundation of Innovation (CFI) for funding. We wish to acknowledge the support of the Natural Sciences and Engineering Research Council of Canada (NSERC) [CREATE 511601-2018].

ACKNOWLEDGMENTS

The authors wish to thank Mr. Emre Yurdusev for his help with preliminary experiments.

ABBREVIATIONS

DNA, deoxyribonucleic acid; RNA, ribonucleic acid; RZ, ribozyme; DMF, digital microfluidics chip; HHR, hammerhead ribozyme; SAV, surface area to volume; LoD, limit of detection; LoQ, limit of quantification; PC, positive control; NC, negative control; AS, assay

REFERENCES

(1) Whitesides, G. M. The Origins and the Future of Microfluidics. *Nature* **2006**, *442*, 368−373.

(2) Manz, A.; Miyahara, Y.; Miura, J.; Watanabe, Y.; Miyagi, H.; Sato, K. Design of an Open-Tubular Column Liquid Chromatograph Using Silicon Chip Technology. *Sens. Actuators, B* **1990**, *1*, 249−255.

(3) Oblath, E. A.; Henley, W. H.; Alarie, J. P.; Ramsey, J. M. A Microfluidic Chip Integrating DNA Extraction and Real-Time PCR for the Detection of Bacteria in Saliva. *Lab Chip* **2013**, *13*, 1325−1332.

(4) Ahmadi, F.; Samlali, K.; Vo, P. Q. N.; Shih, S. C. C. An Integrated Droplet-Digital Microfluidic System for on-Demand Droplet Creation, Mixing, Incubation, and Sorting. *Lab Chip* **2019**, *19*, 524−535.

(5) Nayak, S.; Blumenfeld, N. R.; Laksanasopin, T.; Sia, S. K. Point-of-Care Diagnostics: Recent Developments in a Connected Age. *Anal. Chem.* **2017**, *89*, 102−123.

(6) Hadd, A. G.; Raymond, D. E.; Halliwell, J. W.; Jacobson, S. C.; Ramsey, J. M. Microchip Device for Performing Enzyme Assays. *Anal. Chem.* **1997**, *69*, 3407−3412.

(7) Hadd, A. G.; Jacobson, S. C.; Ramsey, J. M. Microfluidic Assays of Acetylcholinesterase Inhibitors. *Anal. Chem.* **1999**, *71*, 5206−5212.

(8) Burke, B. J.; Regnier, F. E. Stopped-Flow Enzyme Assays on a Chip Using a Microfabricated Mixer. *Anal. Chem.* **2003**, *75*, 1786−1791.

(9) Teh, S.-Y.; Lin, R.; Hung, L.-H.; Lee, A. P. Droplet Microfluidics. *Lab Chip* **2008**, *8*, 198−220.

(10) van Dijke, K. C.; Veldhuis, G.; Schroën, K.; Boom, R. M. Simultaneous Formation of Many Droplets in a Single Microfluidic Droplet Formation Unit. *AIChE J.* **2009**, *56*, 833−836.

(11) Phelan, F. R., Jr.; Hughes, N. R.; Pathak, J. A. Chaotic Mixing in Microfluidic Devices Driven by Oscillatory Cross Flow. *Phys. Fluids* **2008**, *20*, No. 023101.

(12) Lee, J.; Moon, H.; Fowler, J.; Schoellhammer, T.; Kim, C.-J. Electrowetting and Electrowetting-on-Dielectric for Microscale Liquid Handling. *Sens. Actuators, A* **2002**, *95*, 259−268.

(13) Pollack, M. G.; Shenderov, A. D.; Fair, R. B. Electrowetting-Based Actuation of Droplets for Integrated Microfluidics. *Lab Chip* **2002**, 96.

(14) Pollack, M. G.; Fair, R. B.; Shenderov, A. D. Electrowetting-Based Actuation of Liquid Droplets for Microfluidic Applications. *Appl. Phys. Lett.* **2000**, *77*, 1725−1726.

(15) *The Digital Revolution: A New Paradigm for Microfluidics - Abdelgawad - 2009 - Advanced Materials - Wiley Online Library* https://onlinelibrary .wiley.com/doi/abs/10.1002/adma.200802244 (accessed 2020 -09-17).

(16) *Digital bioanalysis | SpringerLink* https://link.springer.com/article/10.1007/s00216-008-2397-x (accessed 2020−09 -17).

(17) Mj, J. J.; Wheeler, A. R. Let's Get Digital: Digitizing Chemical Biology with Microfluidics. *Curr. Opin. Chem. Biol.* **2010**, *14*, 574−581.

(18) Hess, D.; Yang, T.; Stavrakis, S. Droplet-Based Optofluidic Systems for Measuring Enzyme Kinetics. *Anal. Bioanal. Chem.* **2020**, *412*, 3265−3283.

(19) Chang, C.; Sustarich, J.; Bharadwaj, R.; Chandrasekaran, A.; Adams, P. D.; Singh, A. K. Droplet-Based Microfluidic Platform for Heterogeneous Enzymatic Assays. *Lab Chip* **2013**, *13*, 1817−1822.
(20) Cohen, C. B.; Chin-Dixon, E.; Jeong, S.; Nikiforov, T. T. A Microchip-Based Enzyme Assay for Protein Kinase A. *Anal. Biochem.* **1999**, *273*, 89−97.
(21) Agresti, J. J.; Antipov, E.; Abate, A. R.; Ahn, K.; Rowat, A. C.; Baret, J.-C.; Marquez, M.; Klibanov, A. M.; Griffiths, A. D.; Weitz, D. A. Ultrahigh-Throughput Screening in Drop-Based Microfluidics for Directed Evolution. *Proc. Natl. Acad. Sci. U. S. A.* **2010**, *107*, 4004−4009.
(22) Shi, Q.; Qin, L.; Wei, W.; Geng, F.; Fan, R.; Shin, Y. S.; Guo, D.; Hood, L.; Mischel, P. S.; Heath, J. R. Single-Cell Proteomic Chip for Profiling Intracellular Signaling Pathways in Single Tumor Cells. *Proc. Natl. Acad. Sci. U. S. A.* **2012**, *109*, 419−424.
(23) Wei, Z.; Li, Y.; Cooks, R. G.; Yan, X. Accelerated Reaction Kinetics in Microdroplets: Overview and Recent Developments. *Annu. Rev. Phys. Chem.* **2020**, *71*, 31−51.
(24) Boutet, J.; Castellan, G.; Chabrol, C.; Chollat-Namy, A.; Fouillet, Y.; Gasparutto, D.; Jary, D.; Peponnet, C. *DNA repair enzyme analysis on EWOD fluidic microprocessor* https://www.semanticscholar.org/paper/DNA-repair-enzyme-analysis-on-EWOD-fluidic-Boutet-Castellan/3963ed5abf6ef3a60e7ecbc49530e25b4fafd231 (accessed 2020−10 -31).
(25) Miller, E. M.; Wheeler, A. R. A Digital Microfluidic Approach to Homogeneous Enzyme Assays. *Anal. Chem.* **2008**, *80*, 1614−1619.
(26) Leclerc, L. M. Y.; Soffer, G.; Kwan, D. H.; Shih, S. C. C. A Fucosyltransferase Inhibition Assay Using Image-Analysis and Digital Microfluidics. *Biomicrofluidics* **2019**, *13*, No. 034106.
(27) Forster, A. C.; Symons, R. H. Self-Cleavage of plus and Minus RNAs of a Virusoid and a Structural Model for the Active Sites. *Cell* **1987**, *49*, 211−220.
(28) Ouellet, J.; Byrne, M.; Lilley, D. M. J. Formation of an Active Site in *Trans* by Interaction of Two Complete Varkud Satellite Ribozymes. *RNA* **2009**, *15*, 1822−1826.
(29) Mercure, S.; Lafontaine, D.; Ananvoranich, S.; Perreault, J.-P. Kinetic Analysis of δ Ribozyme Cleavage. *Biochemistry* **1998**, *37*, 16975−16982.
(30) Stage-Zimmermann, T. K.; Uhlenbeck, O. C. Hammerhead Ribozyme Kinetics. *RNA* **1998**, *4*, 875−889.
(31) Perreault, J.; Weinberg, Z.; Roth, A.; Popescu, O.; Chartrand, P.; Ferbeyre, G.; Breaker, R. R. Identification of Hammerhead Ribozymes in All Domains of Life Reveals Novel Structural Variations. *PLoS Comput. Biol.* **2011**, *7*, No. e1002031.
(32) Chow, C. S.; Somne, S.; Llano-Sotelo, B. Monitoring Hammerhead Ribozyme-Catalyzed Cleavage with a Fluorescein-Labeled Substrate: Effects of Magnesium Ions and Antibiotic Inhibitors. A Biochemistry Laboratory: Part 2. *J. Chem. Educ.* **1999**, *76*, 651.
(33) Ausländer, S.; Fuchs, D.; Hürlemann, S.; Ausländer, D.; Fussenegger, M. Engineering a Ribozyme Cleavage-Induced Split Fluorescent Aptamer Complementation Assay. *Nucleic Acids Res.* **2016**, *44*, No. e94.
(34) Singh, K. K.; Parwaresch, R.; Krupp, G. Rapid Kinetic Characterization of Hammerhead Ribozymes by Real-Time Monitoring of Fluorescence Resonance Energy Transfer (FRET). *RNA* **1999**, *5*, 1348−1356.
(35) Rossi, J. J. Therapeutic Applications of Ribozymes. In *Nucleic Acid Therapeutics in Cancer*; Gewirtz, A. M., Ed.; Cancer Drug Discovery and Development; Humana Press: Totowa, NJ, 2004; pp. 45−64. doi: DOI: 10.1007/978-1-59259-777-2_4.
(36) Breaker, R. R. Engineered Allosteric Ribozymes as Biosensor Components. *Curr. Opin. Biotechnol.* **2002**, *13*, 31−39.
(37) Penchovsky, R.; Breaker, R. R. Computational Design and Experimental Validation of Oligonucleotide-Sensing Allosteric Ribozymes. *Nat. Biotechnol.* **2005**, *23*, 1424−1433.
(38) Penchovsky, R. Engineering Integrated Digital Circuits with Allosteric Ribozymes for Scaling up Molecular Computation and Diagnostics. *ACS Synth. Biol.* **2012**, *1*, 471−482.
(39) Ryckelynck, M.; Baudrey, S.; Rick, C.; Marin, A.; Coldren, F.; Westhof, E.; Griffiths, A. D. Using Droplet-Based Microfluidics to Improve the Catalytic Properties of RNA under Multiple-Turnover Conditions. *RNA* **2015**, *21*, 458−469.
(40) Hadwen, B.; Broder, G. R.; Morganti, D.; Jacobs, A.; Brown, C.; Hector, J. R.; Kubota, Y.; Morgan, H. Programmable Large Area Digital Microfluidic Array with Integrated Droplet Sensing for Bioassays. *Lab Chip* **2012**, *12*, 3305−3313.
(41) Kim, H.-K.; Chen, S.; Javed, M. R.; Lei, J.; Kim, C.-J.; Keng, P. Y.; van Dam, R. M. Multi-Step Organic Synthesis of Four Different Molecular Probes in Digital Microfluidic Devices. In *Proceedings of International Conference on Miniaturized Systems for Chemistry and Life Sciences (mTAS)* 2012; pp. 617−619.
(42) Fobel, R.; Fobel, C.; Wheeler, A. R. DropBot: An Open-Source Digital Microfluidic Control System with Precise Control of Electrostatic Driving Force and Instantaneous Drop Velocity Measurement. *Appl. Phys. Lett.* **2013**, *102*, 193513.
(43) Vo, P. Q. N.; Husser, M. C.; Ahmadi, F.; Sinha, H.; Shih, S. C. C. Image-Based Feedback and Analysis System for Digital Microfluidics. *Lab Chip* **2017**, *17*, 3437−3446.
(44) Hertel, K. J.; Pardi, A.; Uhlenbeck, O. C.; Koizumi, M.; Ohtsuka, E.; Uesugi, S.; Cedergren, R.; Eckstein, F.; Gerlach, W. L.; Hodgson, R. Numbering System for the Hammerhead. *Nucleic Acids Res.* **1992**, *20*, 3252.
(45) Kuimelis, R. G.; McLaughlin, L. W. Probing the Cleavage Activity of the Hammerhead Ribozyme Using Analog Complexes. In *Catalytic RNA*, Eckstein, F.; Lilley, D. M. J., Eds.; Nucleic Acids and Molecular Biology; Springer: Berlin, Heidelberg, 1997; pp. 197−215, DOI: 10.1007/978-3-642-61202-2_11.
(46) Kapadia, J. B.; Kharma, N.; Davis, A. N.; Kamel, N.; Perreault, J. Measurement of Kinetics of Hammerhead Ribozyme Cleavage Reactions Using Toehold Mediated Strand Displacement. *bioRxiv* **2020**, DOI: 10.1101/2020.09.19.304931.
(47) Beneyton, T.; Thomas, S.; Griffiths, A. D.; Nicaud, J.-M.; Drevelle, A.; Rossignol, T. Droplet-Based Microfluidic High-Throughput Screening of Heterologous Enzymes Secreted by the Yeast *Yarrowia Lipolytica*. *Microb. Cell Fact.* **2017**, *16*, 18.
(48) Lapierre, F.; Gao, Y.; Oakeshott, J.; Peat, T. S.; Zhu, Y. Enzyme Assay in Microfluidics. In *Encyclopedia of Microfluidics and Nanofluidics*, Li, D., Ed.; Springer US: Boston, MA, 2014; pp. 1−8, DOI: 10.1007/978-3-642-27758-0_490-6.
(49) Taniguchi, T.; Torii, T.; Higuchi, T. Chemical Reactions in Microdroplets by Electrostatic Manipulation of Droplets in Liquid Media. *Lab Chip* **2002**, *2*, 19−23.
(50) Skilandat, M.; Sigel, R. K. O. Ribozymes. In *Brenner's Encyclopedia of Genetics* (Second *Edition*); Maloy, S.; Hughes, K., Eds.; Elsevier: San Diego, 2013; pp. 254−258, DOI: 10.1016/B978-0-12-374984-0.01340-1.
(51) Jenne, A.; Hartig, J. S.; Piganeau, N.; Tauer, A.; Samarsky, D. A.; Green, M. R.; Davies, J.; Famulok, M. Rapid Identification and Characterization of Hammerhead-Ribozyme Inhibitors Using Fluorescence-Based Technology. *Nat. Biotechnol.* **2001**, *19*, 56−61.
(52) Singh, K. K.; Rücker, T.; Hanne, A.; Parwaresch, R.; Krupp, G. Fluorescence Polarization for Monitoring Ribozyme Reactions in Real Time. *BioTechniques* **2000**, *29*, 344−351.
(53) Berthier, J.; Peponnet, C. A Model for the Determination of the Dimensions of Dents for Jagged Electrodes in Electrowetting on Dielectric Microsystems. *Biomicrofluidics* **2007**, *1*, No. 014104.
(54) Abdelgawad, M.; Park, P.; Wheeler, A. R. Optimization of Device Geometry in Single-Plate Digital Microfluidics. *J. Appl. Phys.* **2009**, *105*, No. 094506.
(55) Rajabi, N.; Dolatabadi, A. A Novel Electrode Shape for Electrowetting-Based Microfluidics. *Colloids Surf., A* **2010**, *365*, 230−236.
(56) Srinivasan, V.; Pamula, V. K.; Fair, R. B. Droplet-Based Microfluidic Lab-on-a-Chip for Glucose Detection. *Anal. Chim. Acta* **2004**, *507*, 145−150.
(57) Choi, K.; Ng, A. H. C.; Fobel, R.; Wheeler, A. R. Digital Microfluidics. *Annu. Rev. Anal. Chem.* **2012**, *5*, 413−440.

(58) Kwapiszewski, R.; Szczudlowska, J.; Kwapiszewska, K.; Dybko, A.; Brzozka, Z. Effect of Downscaling on the Linearity Range of a Calibration Curve in Spectrofluorimetry. *Anal. Bioanal. Chem.* **2014**, *406*, 4551−4556.
(59) Pennathur, S.; Meinhart, C. D.; Soh, H. T. How to Exploit the Features of Microfluidics Technology. *Lab Chip* **2008**, *8*, 20−22.
(60) Tabaka, M.; Kalwarczyk, T.; Szymanski, J.; Hou, S.; Holyst, R. The Effect of Macromolecular Crowding on Mobility of Biomolecules, Association Kinetics, and Gene Expression in Living Cells. *Front. Phys.* **2014**, *2*, 54.
(61) Sekella, P. T.; Rueda, D.; Walter, N. G. A Biosensor for Theophylline Based on Fluorescence Detection of Ligand-Induced Hammerhead Ribozyme Cleavage. *RNA* **2002**, *8*, 1242−1252.
(62) Penchovsky, R. Computational Design of Allosteric Ribozymes as Molecular Biosensors. *Biotechnol. Adv.* **2014**, *32*, 1015−1027.
(63) Penchovsky, R. Computational Design and Biosensor Applications of Small Molecule-Sensing Allosteric Ribozymes. *Biomacromolecules* **2013**, *14*, 1240−1249.
(64) Gauglitz, G. Analytical Evaluation of Sensor Measurements. *Anal. Bioanal. Chem.* **2018**, *410*, 5−13.
(65) Lavín, Á.; De Vicente, J.; Holgado, M.; Laguna, M. F.; Casquel, R.; Santamaría, B.; Maigler, M. V.; Hernández, A. L.; Ramírez, Y. On the Determination of Uncertainty and Limit of Detection in Label-Free Biosensors. *Sensors* **2018**, *18*, 2038.
(66) Taleuzzaman, M. Limit of Blank (LOB), Limit of Detection (LOD), and Limit of Quantification (LOQ). *Org. Med. Chem. Int. J.* **2018**, *7*, 555722.
(67) Thompson, M.; Ellison, S. L. R.; Wood, R. Harmonized Guidelines for Single-Laboratory Validation of Methods of Analysis (IUPAC Technical Report). *Pure Appl. Chem.* **2002**, 835.
(68) Li, X.; Zhao, C.; Liu, X. A Paper-Based Microfluidic Biosensor Integrating Zinc Oxide Nanowires for Electrochemical Glucose Detection. *Microsyst. Nanoeng.* **2015**, *1*, 15014−15017.
(69) Tian, S.; Das, R. Primerize-2D: Automated Primer Design for RNA Multidimensional Chemical Mapping. *Bioinformatics* **2017**, *33*, 1405.
(70) Samlali, K.; Ahmadi, F.; Quach, A. B. V.; Soffer, G.; Shih, S. C. C. One Cell, One Drop, One Click: Hybrid Microfluidics for Mammalian Single Cell Isolation. *Small* **2020**, *16*, 2002400.
(71) Shih, S. C. C.; Gach, P. C.; Sustarich, J.; Simmons, B. A.; Adams, P. D.; Singh, S.; Singh, A. K. A Droplet-to-Digital (D2D) Microfluidic Device for Single Cell Assays. *Lab Chip* **2015**, *15*, 225−236.

https://doi.org/10.1021/acsomega.1c00239
ACS Omega 2021, 6, 22514−22524